

Structural Control of the Side-Chain Chromophores To Achieve Highly Efficient Nonlinear Optical Polyurethanes

Zhong'an Li,[†] Zhen Li,^{*,‡} Chong'an Di,[‡] Zhichao Zhu,[†] Qianqian Li,[†] Qi Zeng,[†] Kai Zhang,[†] Yunqi Liu,[‡] Cheng Ye,^{*,‡} and Jingui Qin^{*,†}

Hubei Key Lab on Organic and Polymeric Opto-Electronic Materials, Department of Chemistry, Wuhan University, Wuhan 430072, China, and Organic Solids Laboratories, Institute of Chemistry, The Chinese Academy of Sciences, Beijing 100080, China

Received April 20, 2006; Revised Manuscript Received July 30, 2006

ABSTRACT: Two series of polyurethanes (**P1–P10**) containing NLO chromophores as side chains were prepared, in which the size of isolation groups was changed from small atoms to much larger groups such as carbazolyl groups. The polymers were well characterized. The tested NLO properties of the polymers demonstrate that the NLO values and the poling efficiency of the polymers are not always improved with increasing of the size of isolation spacer, and for a given chromophore moiety, there is a suitable isolation group present to boost its microscopic β value to possibly higher macroscopic NLO property efficiently.

Introduction

Organic second-order nonlinear optical (NLO) materials have attracted much attention among scientists for their potential applications in photonics due to their large NLO coefficients, ultrafast response time, and ease of integration.^{1,2} One of the major problems encountered in optimizing organic NLO materials is to efficiently translate the large β values of the organic chromophores into high macroscopic NLO activities of polymers. In the past decades, thanks to the great efforts of scientists, the $\mu\beta$ values of chromophores have been improved by up to 250-fold. The NLO properties of the polymers, however, are only enhanced several times due to strong intermolecular dipole–dipole interactions in the polymeric system, which make the poling-induced noncentrosymmetric alignment of chromophores a daunting task.³ Fortunately, controlling the shape of the chromophore has been proved to be an efficient approach for minimizing this interaction and enhancing the poling efficiency, with spherical shape, proposed by Dalton et al., being the most ideal conformation.⁴ Applying the site isolation principle,⁵ Jen et al. prepared a series of NLO dendrimers and polymers containing dendronized chromophores in the side chains, which demonstrates good NLO properties due to the reduction of intermolecular electrostatic interactions.⁶ Also, the NLO materials covalently linked with chromophores demonstrate advantages such as reduction of chromophore–polymer phase separation, enhanced thermal stability of NLO effects, and the possibility of using covalent attachment to augment external ordering forces.⁷ The poling efficiencies and the macro-scale NLO properties of polymers containing dendronized chromophore as side groups are expected to be heavily related to the subtle difference in architectural design.⁸ Thus, it is needed to study the structure–property relationship in detail. Especially for a given chromophore, there is still very scarce information about how to control its shape to achieve optimized poling efficiency. Or, in other words, we do not know which size, including the length, flexibility, and polarity, of isolation spacer should be adjusted for the certain chromophore moieties to boost

its microscopic β value to possibly higher macroscopic NLO property efficiently.

To deepen the exploration of the fundamental architectural design parameters, based partly on our previous research,⁹ in this work, we tried to study the effect of the different size of isolation spacer on the resultant NLO properties. The common azo chromophores with nitro or sulfonyl moieties as the acceptor were used as the NLO active units in this study since they are easily obtained and widely studied.¹⁰ Ten polymers were synthesized, in which the size of isolation spacer was changed from small atoms such as hydrogen to much larger groups (Schemes 1–3). Polyurethanes were chosen as the polymer backbone, mainly due to their convenient syntheses combined with their moderate glass transition temperature, and the strong secondary forces between polymer chains, which prevent the relaxation of oriented chromophore dipoles.¹¹ The tested NLO properties demonstrate that the NLO values and the poling efficiency of the polymers are not always improved with increasing of the size of the isolation spacer, but also related to the dipole moment, the acceptor strength, the bulk, and the active concentration of the chromophores. Herein, we would like to report the syntheses, characterization, and NLO properties of these polymers.

Experimental Section

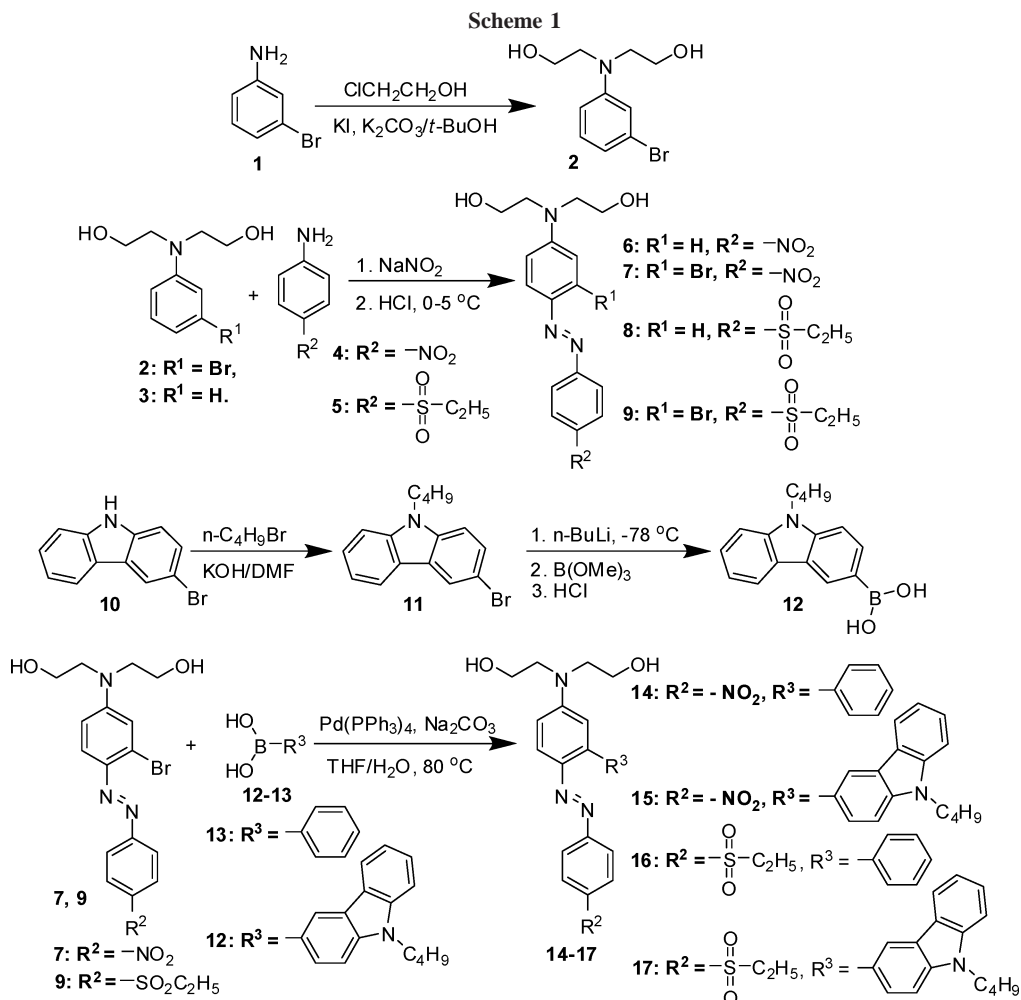
Materials. Tetrahydrofuran (THF) was dried over and distilled from K–Na alloy under an atmosphere of dry nitrogen. *N,N*-Dimethylformamide (DMF) was dried over and distilled from CaH₂ under an atmosphere of dry nitrogen. Toluene 2,4-diisocyanate (TDI) was purified by distillation under reduced pressure before use. 9,9-Dihexylfluorene-2,7-bis(trimethylene borate) (DHFBTMB) was purchased from Aldrich. All other reagents were used as received. 3-Bromocarbazole (**10**) and 4-ethylsulfonylaniline (**5**) was synthesized according to the literature method.¹² 3-Bromo-(2-hydroxyethyl)aminobenzene (**18**) was prepared by the reaction between 3-bromobenzenamine and 2-chloroethanol in water in the presence of sodium hydroxide as the base.

Instrumentation. ¹H and ¹³C NMR spectroscopy study was conducted with a Varian Mercury300 spectrometer using tetramethylsilane (TMS; δ = 0 ppm) as internal standard. The Fourier transform infrared (FTIR) spectra were recorded on a Perkin-Elmer-2 spectrometer in the region of 3000–400 cm^{−1} on KBr pellets. UV–vis spectra were obtained using a Shimadzu 160A

[†] Wuhan University.

[‡] The Chinese Academy of Sciences.

* Corresponding author: Ph 86-27-62254108; Fax 86-27-68756757; e-mail lizhen@whu.edu.cn.



spectrometer. FAB-MS spectra were recorded with a VJ-ZAB-3F mass spectrometer. Elemental analyses were performed by a CARLOERBA-1106 microelemental analyzer. Gel permeation chromatography (GPC) was used to determine the molecular weights of polymers. GPC analysis was performed on a Waters HPLC system equipped with a 2690D separation module and a 2410 refractive index detector. Polystyrene standards were used as calibration standards for GPC. DMF was used as an eluent, and the flow rate was 1.0 mL/min. Thermal analysis was performed on a NETZSCH STA449C thermal analyzer at a heating rate of 20 $^\circ\text{C}/\text{min}$ in nitrogen at a flow rate of 50 cm^3/min for thermogravimetric analysis (TGA). The thermal transitions of the polymers were investigated using a METTLER differential scanning calorimeter DSC822e under nitrogen at a scanning rate of 10 $^\circ\text{C}/\text{min}$. The thermometer for measurement of the melting point was uncorrected. The thickness of the films was measured with an Ambios Technology XP-2 profilometer.

3-Bromo-bis(2-hydroxyethyl)aminobenzene (2). The mixture of 3-bromobenzenamine (**1**) (8.60 g, 0.05 mol) and 2-chloroethanol (13.5 mL, 0.20 mol) was dissolved in *t*-BuOH (100 mL) in the presence of potassium carbonate (21.40 g, 0.16 mol) as an acid acceptor with potassium iodide (1.20 g, 6.8 mmol) as a catalyst. The resultant mixture was stirred at 110 $^\circ\text{C}$ for 9 days. Then the residue was filtered, and most of the solvent was removed under reduced pressure. The crude product was purified with column chromatography on silica gel using ethyl acetate/hexane (4:1) as an eluent to afford white solid (1.40 g, 10.7%); mp = 95–98 $^\circ\text{C}$. ^1H NMR (CDCl_3) δ (ppm): 3.58 (t, $J = 4.8$ Hz, 4H, $-\text{N}-\text{CH}_2-$), 3.88 (t, $J = 4.8$ Hz, 4H, $-\text{O}-\text{CH}_2-$), 6.62 (d, $J = 9.0$ Hz, 1H, ArH), 6.84 (br, 2H, ArH), 7.05 (t, $J = 8.1$ Hz, 1H, ArH).

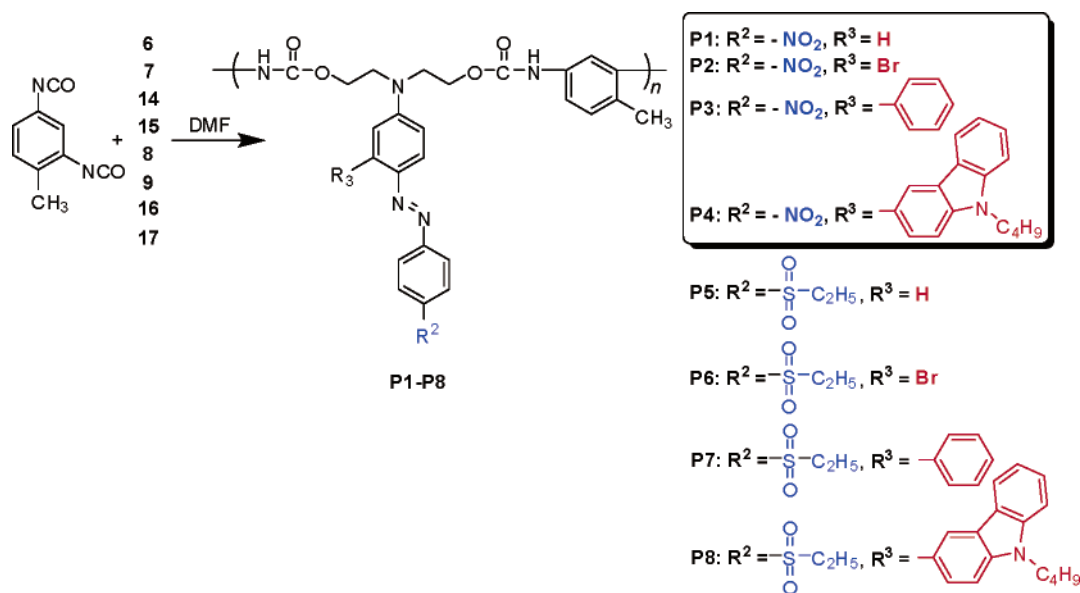
General Procedure for Synthesis of Chromophores 6, 7, 8, 9, 19, and 20. 4-Nitroaniline (**4**) or 4-ethylsulfonylaniline (**5**) (1.00–

1.05 equiv) was dissolved in a water solution of 35% hydrochloric acid. The mixture was cooled to 0–5 $^\circ\text{C}$ in an ice bath, and then a solution of sodium nitrite (1.05 equiv) in water was added dropwise to the above-cooled solution with stirring. After being stirred below 5 $^\circ\text{C}$ for 15 min, a solution of **2**, **3**, or **18** (1.00 equiv) in ethanol was added slowly. The mixture was left in the ice bath for another 1 h, and some sodium bicarbonate was added to adjust the pH value to 7.0. The reaction further stirred for 0.5 h, the deeply red precipitate was filtered, washed with water, and dried in a vacuum desiccator. The crude product was purified by recrystallization or column chromatography.

Chromophore 6. **3** (1.50 g, 8.3 mmol), **4** (1.15 g, 8.3 mmol). Purified by recrystallization from ethanol/water to afford deeply red powder (1.80 g, 65.7%); mp = 205–207 $^\circ\text{C}$. IR (thin film), ν (cm^{-1}): 1601 ($-\text{C}=\text{C}-$), 1512, 1330 ($-\text{NO}_2$). ^1H NMR (acetone- d_6) δ (ppm): 3.75 (t, $J = 5.4$ Hz, 4H, $-\text{N}-\text{CH}_2-$), 3.83 (t, $J = 5.4$ Hz, 4H, $-\text{O}-\text{CH}_2-$), 6.96 (d, $J = 9.3$ Hz, 2H, ArH), 7.88 (d, $J = 9.6$ Hz, 2H, ArH), 8.00 (d, $J = 9.0$ Hz, 2H, ArH), 8.39 (d, $J = 8.7$ Hz, 2H, ArH). UV-vis (THF, 2.5×10^{-5} mol/L): $\lambda_{\text{max}} = 485$ nm; $\epsilon_{\text{max}} = 3.58 \times 10^4$ mol^{-1} L cm^{-1} .

Chromophore 7. **2** (2.00 g, 7.7 mmol), **4** (1.07 g, 7.8 mmol). Purified by recrystallization from ethanol/water to afford deeply red powder (2.23 g, 72.3%); mp = 183–184 $^\circ\text{C}$. IR (thin film), ν (cm^{-1}): 1598 ($-\text{C}=\text{C}-$), 1512, 1333 ($-\text{NO}_2$). ^1H NMR (acetone- d_6) δ (ppm): 3.75 (t, $J = 5.1$ Hz, 4H, $-\text{N}-\text{CH}_2-$), 3.83 (t, $J = 5.4$ Hz, 4H, $-\text{O}-\text{CH}_2-$), 6.95 (dd, $J = 2.7, 9.6$ Hz, 1H, ArH), 7.23 (d, $J = 2.4$ Hz, 1H, ArH), 7.83 (d, $J = 9.3$ Hz, 1H, ArH), 8.04 (d, $J = 9.0$ Hz, 2H, ArH), 8.40 (d, $J = 9.0$ Hz, 2H, ArH). ^{13}C NMR (75 MHz, acetone- d_6) δ (ppm): 54.2, 59.3, 112.1, 115.4, 118.8, 123.1, 125.0, 131.5, 139.6, 148.0, 153.6, 156.8. MS (FAB), m/z [M^+]: 408.5, calcd 408.0. $\text{C}_{16}\text{H}_{17}\text{BrN}_4\text{O}_4$ (EA) (%), found/calcd: C, 46.90/46.96; H, 4.39/4.19; N, 13.41/13.69. UV-vis

Scheme 2



(THF, 2.5×10^{-5} mol/L): $\lambda_{\max} = 479$ nm; $\epsilon_{\max} = 3.97 \times 10^4$ mol $^{-1}$ L cm $^{-1}$.

Chromophore 8. 3 (1.20 g, 6.6 mmol), **5** (1.25 g, 6.7 mmol). Purified by recrystallization from ethanol/water to afford orange red powder (1.71 g, 68.4%); mp = 129–130 °C. IR (thin film), ν (cm $^{-1}$): 1601, 1512 (C=C), 1299, 1131 (SO $_2$). 1 H NMR (acetone- d_6) δ (ppm): 1.3 (t, $J = 7.5$ Hz, 3H, -CH $_3$), 3.15 (q, $J = 7.5$ Hz, 2H, -SO $_2$ CH $_2$ -), 3.75 (t, $J = 5.1$ Hz, 4H, -N-CH $_2$ -), 3.97 (t, $J = 5.1$ Hz, 4H, -O-CH $_2$ -), 6.80 (d, $J = 9.0$ Hz, 2H, ArH), 7.89 (d, $J = 8.7$ Hz, 2H, ArH), 7.98 (q, 4H, ArH). UV-vis (THF, 2.5×10^{-5} mol/L): $\lambda_{\max} = 448$ nm; $\epsilon_{\max} = 3.62 \times 10^4$ mol $^{-1}$ L cm $^{-1}$.

Chromophore 9. 2 (0.78 g, 3.0 mmol), **5** (0.58 g, 3.1 mmol). Purified by recrystallization from ethanol/water to afford orange red powder (1.05 g, 76.6%); mp = 139–140 °C. IR (thin film), ν (cm $^{-1}$): 1592, 1504 (C=C), 1299, 1128 (SO $_2$). 1 H NMR (CDCl $_3$) δ (ppm): 1.30 (t, $J = 7.2$ Hz, 3H, -CH $_3$), 3.15 (q, $J = 7.2$ Hz, 2H, -SO $_2$ CH $_2$ -), 3.72 (br, s, 4H, -N-CH $_2$ -), 3.96 (br, s, 4H, -O-CH $_2$ -), 6.70 (d, $J = 9.0$ Hz, 1H, ArH), 7.04 (s, 1H, ArH), 7.76 (d, $J = 7.2$ Hz, 1H, ArH), 8.01 (m, 4H, ArH). 13 C NMR (75 MHz, CDCl $_3$) δ (ppm): 7.7, 51.0, 55.2, 60.6, 112.0, 116.0, 118.9, 123.5, 129.5, 131.3, 138.5, 140.5, 152.2, 156.2. MS (FAB), m/z [M^+]: 455.3, calcd 455.1. C $_{18}$ H $_{22}$ BrN $_3$ O $_4$ S (EA) (%), found/calcd): C, 47.76/47.37; H, 4.36/4.86; N, 9.15/9.21; S, 6.97/7.03. UV-vis (THF, 2.5×10^{-5} mol/L): $\lambda_{\max} = 449$ nm; $\epsilon_{\max} = 2.98 \times 10^4$ mol $^{-1}$ L cm $^{-1}$.

Chromophore 19. 18 (3.94 g, 18.2 mmol), **4** (2.53 g, 18.3 mmol). Purified by recrystallization from acetone/water to afford deeply red powder (4.52 g, 68.1%); mp = 170–171 °C. 1 H NMR (acetone- d_6) δ (ppm): 3.43 (t, $J = 5.4$ Hz, 2H, -N-CH $_2$ -), 3.79 (t, $J = 5.4$ Hz, 2H, -O-CH $_2$ -), 6.82 (dd, $J = 2.7, 9.0$ Hz, 1H, ArH), 7.13 (d, $J = 2.7$ Hz, 1H, ArH), 7.81 (d, $J = 8.7$ Hz, 1H, ArH), 8.03 (d, $J = 9.3$ Hz, 2H, ArH), 8.40 (d, $J = 9.0$ Hz, 2H, ArH).

Chromophore 20. 18 (0.76 g, 3.5 mmol), **5** (0.65 g, 3.5 mmol). Purified by column chromatography on silica gel using ethyl acetate/hexane (3/1) as an eluent to afford red powder (0.60 g, 42.0%); mp = 67–70 °C. 1 H NMR (CDCl $_3$) δ (ppm): 1.20 (t, $J = 7.8$ Hz, 3H, -CH $_3$), 3.07 (q, $J = 7.5$ Hz, 2H, -SO $_2$ CH $_2$ -), 3.33 (t, $J = 5.1$ Hz, 2H, -N-CH $_2$ -), 3.95 (br, s, 2H, -O-CH $_2$ -), 6.54 (d, $J = 9.0$ Hz, 1H, ArH), 6.91 (s, 1H, ArH), 7.71 (d, $J = 7.8$ Hz, 1H, ArH), 8.02 (m, 4H, ArH).

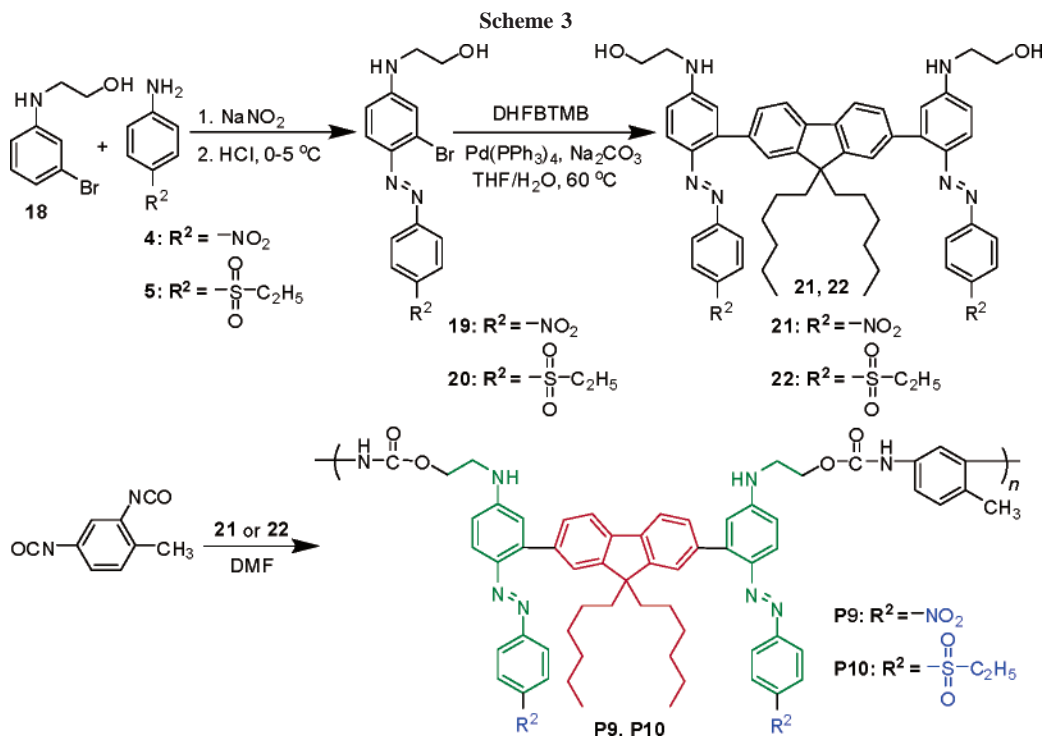
Synthesis of *N*-(*n*-Butane)-3-bromocarbazole (11). 3-Bromocarbazole (**10**) (0.80 g, 3.2 mmol) was dissolved in DMF (12 mL), and then powdered potassium hydroxide (0.91 g, 16.2 mmol) was added. After the mixture was stirred for 1 h, the solution of 1-bromobutane (0.89 g, 6.5 mmol) was added slowly. After stirred for 20 h at room temperature, the mixture was poured into ice water

(200 mL), then extracted with chloroform, and washed with water. The organic layer was dried over magnesium sulfate. The crude product was purified with column chromatography on silica gel using chloroform/hexane (1/2) as eluent to afford the colorless oil (0.91 g, 92.3%). 1 H NMR (CDCl $_3$) δ (ppm): 0.96 (t, $J = 6.6$ Hz, 3H, -CH $_3$), 1.40 (m, 2H, -CH $_2$ CH $_3$), 1.85 (m, 2H, -CH $_2$ -CH $_2$ -), 4.30 (t, $J = 6.6$ Hz, 2H, -N-CH $_2$ -), 7.25 (m, 2H, ArH), 7.40–7.55 (m, 3H, ArH), 8.08 (d, $J = 7.2$ Hz, 1H, ArH), 8.21 (s, 1H, ArH).

Synthesis of 3-*N*-(*n*-Butane)carbazole Boronic Acid (12). A solution of **11** (0.90 g, 3.0 mmol) in THF (5 mL) was added dropwise to a solution of *n*-BuLi (2.0 mL, 3.3 mmol, 1.64 M in *n*-hexane, Aldrich) in THF (10 mL) at -78 °C under nitrogen, the mixture was stirred for 1 h, then trimethyl borate (0.66 g, 6.3 mmol) was added dropwise, and the reaction mixture was stirred for another 1 h at -78 °C and then stirred overnight at room temperature. Hydrochloric acid (2 M) (7.2 mL) was then added into the mixture, and the mixture was stirred for 30 min. The resultant mixture was extracted with ether and washed with distilled water three times. The organic layer was dried over magnesium sulfate and evaporated to dryness. The crude product was dissolved in ether and dropped into 20 mL of *n*-hexane, then filtered, and washed with *n*-hexane to afford white solid (0.27 g, 34.0%). 1 H NMR (CDCl $_3$) δ (ppm): 1.01 (t, $J = 7.2$ Hz, 3H, -CH $_3$), 1.45 (m, 2H, -CH $_2$ CH $_3$), 1.93 (m, 2H, -CH $_2$ -CH $_2$ -), 4.41 (t, $J = 7.5$ Hz, 2H, -N-CH $_2$ -), 7.35 (m, 1H, ArH), 7.4–7.6 (m, 3H, ArH), 8.37 (d, $J = 7.8$ Hz, 1H, ArH), 8.50 (d, $J = 8.4$ Hz, 1H, ArH), 9.13 (s, 1H, ArH).

General Procedure for Synthesis of Chromophores 14, 15, 16, and 17 through Suzuki Reaction. A mixture of chromophores **7** or **9** (1.00 equiv), the boronic acid **12** or **13** (0.90–1.10 equiv), sodium carbonate (10.0 equiv), THF (monomer concentration is about 0.025 M)/water (3:1 in volume), and tetrakis(triphenylphosphine)palladium Pd(PPh $_3$) $_4$ (3–5 mol %) was carefully degassed and charged with nitrogen. The reaction was stirred for 18–30 h at 80 °C. After it was cooled to room temperature, the organic layer was separated, dried over sodium sulfate, and evaporated to dryness. The crude product was purified by recrystallization or column chromatography.

Chromophore 14. 7 (0.35 g, 0.86 mmol), **13** (0.11 g, 0.90 mmol). Purified by recrystallization from acetone to afford deeply red powder (0.23 g, 66.4%); mp = 121–123 °C. IR (thin film), ν (cm $^{-1}$): 1595 (C=C), 1512, 1333 (NO $_2$). 1 H NMR (acetone- d_6) δ (ppm): 3.81 (t, $J = 4.8$ Hz, 4H, -N-CH $_2$ -), 3.88 (t, $J = 5.1$ Hz, 4H, -O-CH $_2$ -), 6.94 (s, 1H, ArH), 6.98 (d, $J = 9.3$ Hz, 1H, ArH), 7.47 (m, 3H, ArH), 7.57 (d, $J = 6.9$ Hz, 2H, ArH), 7.81 (d, $J = 9.3$ Hz, 2H, ArH), 7.97 (d, $J = 9.0$ Hz, 1H, ArH), 8.31 (d, $J = 8.7$ Hz, 2H, ArH). 13 C NMR (75 MHz, acetone- d_6) δ (ppm):



54.3, 59.5, 112.2, 112.7, 117.5, 122.9, 124.9, 127.5, 127.7, 131.0, 140.0, 140.5, 146.4, 147.5, 152.7, 157.0. MS (FAB), m/z [M^+]: 406.5, calcd, 406.2. $C_{22}H_{22}N_4O_4$ (EA) (%), found/calcd: C, 65.31/65.01; H, 5.58/5.46; N, 13.27/13.78. UV-vis (THF, 2.5×10^{-5} mol/L): $\lambda_{max} = 487$ nm; $\epsilon_{max} = 3.03 \times 10^4$ mol $^{-1}$ L cm $^{-1}$.

Chromophore 15. 7 (0.20 g, 0.49 mmol), **12** (0.12 g, 0.45 mmol). Purified by column chromatography on silica gel using 3/1 ethyl acetate/hexane to afford deeply red powder (0.22 g, 81.0%); mp = 110–112 °C. IR (thin film), ν (cm $^{-1}$): 1595 (C=C), 1513, 1333 (–NO $_2$). 1H NMR (CDCl $_3$) δ (ppm): 1.00 (t, $J = 7.2$ Hz, 3H, –CH $_3$), 1.46 (m, 2H, –CH $_2$ CH $_3$), 1.92 (m, 2H, –CH $_2$ –CH $_2$ –), 3.82 (br, s, 4H, –N–CH $_2$ –), 4.02 (br, s, 4H, –O–CH $_2$ –), 4.37 (t, $J = 7.2$ Hz, 2H, –N–CH $_2$ –), 6.79 (d, $J = 7.2$ Hz, 1H, ArH), 6.92 (s, 1H, ArH), 7.23 (m, 1H, ArH), 7.48 (m, 3H, ArH), 7.60 (d, 1H, ArH), 7.75 (d, $J = 8.7$ Hz, 2H, ArH), 7.97 (d, $J = 8.7$ Hz, 1H, ArH), 8.03 (d, $J = 7.2$ Hz, 1H, ArH), 8.18 (m, 3H, ArH). ^{13}C NMR (75 MHz, CDCl $_3$) δ (ppm): 14.1, 20.8, 31.4, 43.3, 55.5, 61.0, 108.0, 109.2, 111.9, 113.7, 117.8, 119.3, 120.4, 122.6, 123.2, 124.9, 126.1, 128.9, 130.0, 140.3, 141.1, 141.6, 147.0, 147.4, 151.6, 157.0. MS (FAB), m/z [M^+]: 550.5, calcd, 551.3. $C_{32}H_{33}N_5O_4$ (EA) (%), found/calcd: C, 69.05/69.67; H, 6.34/6.03; N, 12.45/12.70. UV-vis (THF, 2.5×10^{-5} mol/L): $\lambda_{max} = 491$ nm; $\epsilon_{max} = 3.50 \times 10^4$ mol $^{-1}$ L cm $^{-1}$.

Chromophore 16. 9 (0.40 g, 0.88 mmol), **13** (0.12 g, 0.97 mmol). Purified by recrystallization from acetone to afford red powder (0.29 g, 73.6%); mp = 180–181 °C. IR (thin film), ν (cm $^{-1}$): 1595, 1497 (C=C), 1299, 1125 (–SO $_2$). 1H NMR (acetone- d_6) δ (ppm): 1.20 (t, $J = 7.2$ Hz, 3H, –CH $_3$), 3.22 (q, $J = 7.2$ Hz, 2H, –SO $_2$ CH $_2$ –), 3.79 (t, $J = 5.1$ Hz, 4H, –N–CH $_2$ –), 3.85 (t, $J = 5.1$ Hz, 4H, –O–CH $_2$ –), 6.91 (s, 1H, ArH), 6.95 (d, $J = 9.0$ Hz, 1H, ArH), 7.46 (m, 3H, ArH), 7.55 (d, $J = 7.2$ Hz, 2H, ArH), 7.83 (d, $J = 8.1$ Hz, 2H, ArH), 7.94 (m, 3H, ArH). ^{13}C NMR (75 MHz, acetone- d_6) δ (ppm): 7.0, 50.1, 54.3, 59.5, 112.1, 112.7, 117.3, 122.8, 127.4, 127.7, 129.4, 131.0, 138.8, 140.1, 140.4, 146.0, 152.3, 156.5. MS (FAB), m/z [M^+]: 453.6, calcd, 453.2. $C_{24}H_{27}N_3O_4S$ (EA) (%), found/calcd: C, 63.50/63.56; H, 6.12/6.00; N, 9.23/9.26; S, 7.16/7.07. UV-vis (THF, 2.5×10^{-5} mol/L): $\lambda_{max} = 452$ nm; $\epsilon_{max} = 2.88 \times 10^4$ mol $^{-1}$ L cm $^{-1}$.

Chromophore 17. 9 (0.23 g, 0.50 mmol), **12** (0.13 g, 0.49 mmol). Purified by column chromatography on silica gel using ethyl acetate/hexane (4/1) as an eluent to afford red powder (0.27 g, 90.0%); mp = 96–98 °C. IR (thin film), ν (cm $^{-1}$): 1595, 1495

(C=C), 1299, 1125 (–SO $_2$). 1H NMR (CDCl $_3$) δ (ppm): 0.97 (t, $J = 7.5$ Hz, 3H, –CH $_3$), 1.21 (t, $J = 7.5$ Hz, 3H, –SO $_2$ CH $_2$ –CH $_3$ –), 1.48 (m, 2H, –CH $_2$ CH $_3$), 1.90 (m, 2H, –CH $_2$ CH $_2$ –), 3.05 (q, $J = 7.2$ Hz, 2H, –SO $_2$ CH $_2$ –), 3.82 (br, s, 4H, –N–CH $_2$ –), 4.02 (br, s, 4H, –O–CH $_2$ –), 4.36 (t, $J = 7.2$ Hz, 2H, –N–CH $_2$ –), 6.83 (d, $J = 7.5$ Hz, 1H, ArH), 6.92 (s, 1H, ArH), 7.20 (m, 1H, ArH), 7.46 (m, 3H, ArH), 7.58 (d, 1H, ArH), 7.8 (br, s, 4H, ArH), 8.01 (d, 2H, ArH), 8.19 (s, 1H, ArH). ^{13}C NMR (75 MHz, CDCl $_3$) δ (ppm): 7.6, 14.1, 20.8, 31.4, 43.2, 50.9, 55.4, 61.0, 107.9, 109.1, 111.9, 113.6, 117.7, 119.3, 120.4, 122.6, 123.0, 123.1, 123.2, 126.0, 129.0, 129.4, 130.1, 137.7, 140.3, 141.1, 141.5, 146.7, 151.4, 156.7. MS (FAB), m/z [M^+]: 598.0, calcd, 598.3. $C_{34}H_{38}N_4O_4S$ (EA) (%), found/calcd: C, 68.13/68.20; H, 6.69/6.40; N, 9.40/9.36; S, 0.532/5.36. UV-vis (THF, 2.5×10^{-5} mol/L): $\lambda_{max} = 456$ nm; $\epsilon_{max} = 1.80 \times 10^4$ mol $^{-1}$ L cm $^{-1}$.

General Procedure for Synthesis of Chromophores 21 and 22 through Suzuki Reaction. A mixture of chromophore **19** or **20** (1.00 equiv), 9,9-dihexylfluorene-2,7-bis(trimethyleneborate) (Aldrich) (0.49 equiv), sodium carbonate (10.0 equiv), THF (monomer concentration is about 0.025 M)/water (3:1 in volume), and Pd(PPh $_3$) $_4$ (3–5 mol %) was carefully degassed and charged with nitrogen. The reaction mixture stirred for 30 h at 80 °C. After it was cooled to room temperature, the organic layer was separated, dried over Na $_2$ SO $_4$, and evaporated to dryness. The crude product was purified by recrystallization or column chromatography.

Chromophore 21. 19 (0.21 g, 0.57 mmol), 9,9-dihexylfluorene-2,7-bis(trimethyleneborate) (0.14 g, 0.28 mmol). Purified by column chromatography on silica gel using ethyl acetate/hexane (3/1) as eluent and then recrystallization from acetone to afford deeply red powder (0.19 g, 78.7%); mp = 233–234 °C. IR (thin film), ν (cm $^{-1}$): 1601 (C=C), 1515, 1333 (–NO $_2$). 1H NMR (acetone- d_6) δ (ppm): 0.67 (t, $J = 7.2$ Hz, 6H, –CH $_3$), 1.03 (m, 16H, –(CH $_2$) $_4$ –), 2.06 (m, 4H, –C–CH $_2$ –), 3.48 (t, $J = 5.4$ Hz, 4H, –N–CH $_2$ –), 3.83 (t, $J = 5.4$ Hz, 4H, –O–CH $_2$ –), 6.81 (d, 4H, ArH), 7.61 (m, 4H, ArH), 7.83 (d, $J = 9.0$ Hz, 4H, ArH), 7.97 (m, 4H, ArH), 8.30 (d, $J = 9.0$ Hz, 4H, ArH). ^{13}C NMR (75 MHz, acetone- d_6) δ (ppm): 13.4, 22.4, 24.2, 29.8, 31.6, 39.9, 45.7, 55.1, 60.4, 112.7, 117.9, 119.2, 122.8, 124.7, 125.9, 129.6, 139.1, 140.2, 141.7, 147.2, 147.4, 150.6, 153.6, 157.2. MS (FAB), m/z [M^+]: 903.0, calcd, 902.5. $C_{53}H_{58}N_8O_6$ (EA) (%), found/calcd: C, 68.98/70.19; H, 6.88/6.47; N, 11.44/12.41. UV-vis (THF, 2.5×10^{-5} mol/L): $\lambda_{max} = 469$ nm; $\epsilon_{max} = 5.32 \times 10^4$ mol $^{-1}$ L cm $^{-1}$.

Chromophore 22. 20 (0.40 g, 0.97 mmol), 9,9-dihexylfluorene-2,7-bis(trimethyleneborate) (0.24 g, 4.70 mmol). This was purified by column chromatography on silica gel using ethyl acetate/hexane (2/1) as eluent to afford red powder (0.26 g, 57.1%); mp = 128–131 °C. IR (thin film), ν (cm⁻¹): 1601, 1522 (–C=C–), 1299, 1125 (–SO₂). ¹H NMR (CDCl₃) δ (ppm): 0.68 (t, J = 6.6 Hz, 6H, –CH₂CH₃), 1.03 (m, 16H, –(CH₂)₄–), 1.27 (t, J = 7.5 Hz, 6H, –SO₂CH₂CH₃–), 1.96 (m, 4H, –C–CH₂–), 3.08 (q, 4H, J = 7.5 Hz, –SO₂CH₂–), 3.47 (br, s, 4H, –N–CH₂–), 3.93 (br, s, 4H, –O–CH₂–), 6.71 (m, 4H, ArH), 7.48 (m, 4H, ArH), 7.90 (m, 12H, ArH). ¹³C NMR (75 MHz, CDCl₃) δ (ppm): 7.6, 14.2, 22.7, 24.2, 30.0, 31.7, 40.2, 45.6, 50.9, 55.3, 61.3, 112.8, 113.6, 118.1, 119.1, 123.3, 125.5, 129.4, 130.1, 138.0, 138.5, 140.2, 142.3, 146.7, 150.8, 151.8, 156.4. UV–vis (THF, 2.5 \times 10⁻⁵ mol/L): λ_{max} = 439 nm; ϵ_{max} = 4.08 \times 10⁴ mol⁻¹ L cm⁻¹.

General Procedure for the Synthesis of Polyurethanes P1–P10. NLO chromophore and TDI with equivalent molar ratios were reacted in appropriate anhydrous DMF solution at 80 °C for 12–30 h in an atmosphere of dry nitrogen. After the solution was cooled to ambient temperature, it was dropped into methanol to remove monomer. The polymer was filtered and dried in a vacuum desiccator.

P1. Chromophore **6** (0.185 g, 0.56 mmol), TDI (0.097 g, 0.56 mmol). Deeply red powder (0.060 g, 21.3%). M_w = 12 900, M_w/M_n = 1.16 (GPC, polystyrene calibration). IR (thin film), ν (cm⁻¹): 1724 (C=O), 1592 (–C=C–), 1521, 1333 (–NO₂). ¹H NMR (DMSO-*d*₆) δ (ppm): 2.0 (–CH₃), 3.7–3.9 (–N–CH₂–), 4.2–4.3 (–O–CH₂–), 6.9–7.1 (ArH), 7.5 (ArH), 7.7–8.0 (ArH), 8.3 (ArH), 8.8–9.0 (–NH–), 9.5–9.7 (–NH–). UV–vis (THF, 0.02 mg/mL): λ_{max} (nm) = 473.

P2. Chromophore **7** (0.445 g, 1.09 mmol), TDI (0.190 g, 1.09 mmol). Deeply red powder (0.320 g, 50.4%). M_w = 11 400, M_w/M_n = 1.16 (GPC, polystyrene calibration). IR (thin film), ν (cm⁻¹): 1716 (C=O), 1599 (–C=C–), 1514, 1338 (–NO₂). ¹H NMR (DMSO-*d*₆) δ (ppm): 2.1 (–CH₃), 3.7–3.9 (–N–CH₂–), 4.2–4.3 (–O–CH₂–), 6.9–7.3 (ArH), 7.5 (ArH), 7.7 (ArH), 7.8–8.0 (ArH), 8.3–8.4 (ArH), 8.8–9.0 (–NH–), 9.5–9.7 (–NH–). UV–vis (THF, 0.02 mg/mL): λ_{max} (nm) = 464.

P3. Chromophore **14** (0.192 g, 0.47 mmol), TDI (0.082 g, 0.47 mmol). Deeply red powder (0.110 g, 40.1%). M_w = 11 500, M_w/M_n = 1.13 (GPC, polystyrene calibration). IR (thin film), ν (cm⁻¹): 1726 (C=O), 1596 (–C=C–), 1518, 1334 (–NO₂). ¹H NMR (DMSO-*d*₆) δ (ppm): 2.1 (–CH₃), 3.7–3.9 (–N–CH₂–), 4.2–4.3 (–O–CH₂–), 6.8–7.2 (ArH), 7.3–7.6 (ArH), 7.7 (ArH), 7.9 (ArH), 8.26 (ArH), 8.8–9.0 (–NH–), 9.5–9.7 (–NH–). UV–vis (THF, 0.02 mg/mL): λ_{max} (nm) = 473.

P4. Chromophore **15** (0.166 g, 0.30 mmol), TDI (0.053 g, 0.30 mmol). Deeply red powder (0.095 g, 43.4%). M_w = 10 100, M_w/M_n = 1.13 (GPC, polystyrene calibration). IR (thin film), ν (cm⁻¹): 1724 (C=O), 1596 (–C=C–), 1514, 1331 (–NO₂). ¹H NMR (DMSO-*d*₆) δ (ppm): 0.8–0.9 (–CH₃), 1.2–1.4 (–CH₂CH₃), 1.9–2.2 (–CH₂– and –CH₃), 3.8–4.0 (–N–CH₂–), 4.2–4.5 (–O–CH₂– and –N–CH₂–), 6.9–7.3 (ArH), 7.3–7.8 (ArH), 7.8–8.0 (ArH), 8.0–8.4 (ArH), 8.8–9.0 (–NH–), 9.5–9.7 (–NH–). UV–vis (THF, 0.02 mg/mL): λ_{max} (nm) = 481.

P5. Chromophore **8** (0.457 g, 1.26 mmol), TDI (0.220 g, 1.26 mmol). Orange red powder (0.550 g, 81.2%). M_w = 29 600, M_w/M_n = 1.36 (GPC, polystyrene calibration). IR (thin film), ν (cm⁻¹): 1723 (C=O), 1601 (–C=C–), 1305, 1128 (–SO₂). ¹H NMR (DMSO-*d*₆) δ (ppm): 1.1 (–CH₂CH₃), 2.0 (–CH₃), 3.7–3.9 (–N–CH₂–), 4.2–4.3 (–O–CH₂–), 6.9–7.1 (ArH), 7.5 (ArH), 7.8 (ArH), 7.9–8.0 (ArH), 8.8–9.0 (–NH–), 9.5–9.7 (–NH–). UV–vis (THF, 0.02 mg/mL): λ_{max} (nm) = 437.

P6. Chromophore **9** (0.228 g, 0.5 mmol), TDI (0.089 g, 0.51 mmol). Orange red powder (0.167 g, 52.7%). M_w = 14 900, M_w/M_n = 1.18 (GPC, polystyrene calibration). IR (thin film), ν (cm⁻¹): 1720 (C=O), 1595 (–C=C–), 1298, 1128 (–SO₂). ¹H NMR (DMSO-*d*₆) δ (ppm): 1.1 (–CH₂CH₃), 2.1 (–CH₃), 3.7–3.9 (–N–CH₂–), 4.2–4.3 (–O–CH₂–), 6.9–7.3 (ArH), 7.5 (ArH), 7.7 (ArH), 7.9–8.0 (ArH), 8.8–9.0 (–NH–), 9.5–9.7 (–NH–). UV–vis (THF, 0.02 mg/mL): λ_{max} (nm) = 442.

Table 1. Synthesis of 2

no.	solvent	base	cat.	T (°C)	time (h)	yield (%)
1	H ₂ O	NaOH		120	24	trace ^a
2	no ^b	NaOH	KI	100	168	0 ^c
3	DMF	K ₂ CO ₃	KI	100	360	19.2 ^d
4	<i>t</i> -BuOH	K ₂ CO ₃	KI	110	216	10.7
5	THF	NaH	15-crown-5	80	72	0 ^e

^a The isolated product is almost the monosubstituted compound (**19**).

^b Solid-phase reaction. ^c The reaction was followed by the thin-layer chromatography (TLC), and there was little disubstituted compound **2** detected after 72 h reaction, but no product was obtained after 1 week reaction. ^d The product is difficult to purify, and there are some dark moieties present. ^e Neither monosubstituted compound **18** nor disubstituted compound **2** was detected after 72 h reaction.

P7. Chromophore **16** (0.226 g, 0.5 mmol), TDI (0.090 g, 0.51 mmol). Orange red powder (0.141 g, 43.2%). M_w = 6200, M_w/M_n = 1.27 (GPC, polystyrene calibration). IR (thin film), ν (cm⁻¹): 1723 (C=O), 1595 (–C=C–), 1298, 1125 (–SO₂). ¹H NMR (DMSO-*d*₆) δ (ppm): 1.2 (–CH₂CH₃), 2.1 (–CH₃), 3.8–3.9 (–N–CH₂–), 4.2–4.4 (–O–CH₂–), 6.7–7.2 (ArH), 7.3–7.6 (ArH), 7.7–8.0 (ArH), 8.8–9.0 (–NH–), 9.5–9.7 (–NH–). UV–vis (THF, 0.02 mg/mL): λ_{max} (nm) = 449.

P8. Chromophore **17** (0.209 g, 0.35 mmol), TDI (0.062 g, 0.35 mmol). Orange red powder (0.141 g, 52.0%). M_w = 10 900, M_w/M_n = 1.12 (GPC, polystyrene calibration). IR (thin film), ν (cm⁻¹): 1725 (C=O), 1595 (–C=C–), 1295, 1120 (–SO₂). ¹H NMR (DMSO-*d*₆) δ (ppm): 0.8–1.0 (–CH₃), 1.1 (–SO₂CH₂CH₃–), 1.4 (–CH₂–), 1.8–2.1 (–CH₂– and –CH₃), 3.8–4.0 (–N–CH₂–), 4.3–4.5 (–O–CH₂– and –N–CH₂–), 6.9–7.2 (ArH), 7.3–7.7 (ArH), 7.7–7.9 (ArH), 8.1 (ArH), 8.3 (ArH), 8.8–9.0 (–NH–), 9.5–9.7 (–NH–). UV–vis (THF, 0.02 mg/mL): λ_{max} (nm) = 449.

P9. Chromophore **21** (0.174 g, 0.19 mmol), TDI (0.034 g, 0.19 mmol). Deeply red powder (0.040 g, 19.4%). M_w = 12 600, M_w/M_n = 1.17 (GPC, polystyrene calibration). IR (thin film), ν (cm⁻¹): 1720 (C=O), 1600 (–C=C–), 1514, 1331 (–NO₂). ¹H NMR (DMSO-*d*₆) δ (ppm): 0.6–1.0 (–CH₃), 1.0–1.4 (–CH₂)₄–, 1.9–2.2 (–C–CH₂– and –CH₃), 3.6–3.8 (–N–CH₂–), 4.2–4.4 (–O–CH₂–), 6.7–7.0 (ArH), 7.0–7.4 (ArH), 7.5–8.0 (ArH), 8.2–8.4 (ArH), 8.9–9.1 (–NH–), 9.6–9.8 (–NH–). UV–vis (THF, 0.02 mg/mL): λ_{max} (nm) = 463.

P10. Chromophore **22** (0.217 g, 0.22 mmol), TDI (0.040 g, 0.22 mmol). Orange red powder (0.110 g, 43.0%). M_w = 14 500, M_w/M_n = 1.18 (GPC, polystyrene calibration). IR (thin film), ν (cm⁻¹): 1723 (C=O), 1601 (–C=C–), 1298, 1134 (–SO₂). ¹H NMR (DMSO-*d*₆) δ (ppm): 0.6–0.8 (–CH₃), 0.8–1.2 (–(CH₂)₄–), 1.3 (–SO₂CH₂CH₃–), 1.9–2.2 (–C–CH₂– and –CH₃), 3.5–3.7 (–N–CH₂–), 4.2–4.4 (–O–CH₂–), 6.7–6.9 (ArH), 7.0–7.3 (ArH), 7.4–7.6 (ArH), 7.7–8.0 (ArH), 8.9–9.1 (–NH–), 9.6–9.8 (–NH–). UV–vis (THF, 0.02 mg/mL): λ_{max} (nm) = 437.

Preparation of Polymer Thin Films. The polymers were dissolved in THF (concentration ~4 wt %), and the solutions were filtered through syringe filters. Polymer films were spin-coated onto indium–tin oxide (ITO)-coated glass substrates, which were cleaned by *N,N*-dimethylformide, acetone, distilled water, and THF sequentially in an ultrasonic bath before use. Residual solvent was removed by heating the films in a vacuum oven at 40 °C.

NLO Measurement of Poled Films. The second-order optical nonlinearity of the polymers was determined by in-situ second harmonic generation (SHG) experiment using a closed temperature-controlled oven with optical windows and three needle electrodes. The films were kept at 45° to the incident beam and poled inside the oven, and the SHG intensity was monitored simultaneously. Poling conditions were as follows: temperature: different for each polymer (Table 2); voltage: 7.5 kV at the needle point; gap distance: 0.8 cm. The SHG measurements were carried out with a Nd:YAG laser operating at a 10 Hz repetition rate and an 8 ns pulse width at 1064 nm. A Y-cut quartz crystal served as the reference.

Table 2. Polymerization Results and Characterization Data

no.	yield (%)	M_w^a	M_w/M_n^a	λ_{\max}^b (nm)	T_g^c (°C)	T_d^d (°C)	T^e (°C)	l_s^f (μm)	d_{33}^g (pm/V)	$d_{33(\infty)}^h$ (pm/V)	Φ^i
P1	21.3	12 900	1.16	473 (485)	150	243	169	0.38	56.4	9.5	0.15
P2	50.4	11 400	1.16	464 (479)	140	272	159	0.39	51.9	10.1	0.18
P3	40.1	11 500	1.13	473 (487)	131	258	149	0.42	49.4	8.3	0.20
P4	43.4	10 100	1.13	481 (491)	140	283	157	0.31	82.3	12.0	0.34
P5	81.2	29 600	1.36	437 (448)	125	264	148	0.40	35.9	9.7	0.14
P6	52.7	14 900	1.18	442 (449)	146	269	150	0.51	29.1	7.5	0.14
P7	43.2	6 200	1.27	449 (452)	98	185	90	0.26	63.0	14.9	0.31
P8	52.0	10 900	1.12	449 (456)	131	288	149	0.45	16.1	3.8	0.23
P9	19.4	12 600	1.17	463 (469)			99	0.61	56.0	11.0	0.31
P10	43.0	14 500	1.18	437 (439)	140	272	154	0.91	12.1	3.3	0.18

^a Determined by GPC in DMF on the basis of a polystyrene calibration. ^b The maximum absorption wavelength of polymer solutions in THF, while the maximum absorption wavelength of the corresponding small chromophore molecules in diluted THF solutions are given in parentheses. ^c Glass transition temperature (T_g) of polymers detected by the DSC analyses under nitrogen at a heating rate of 10 °C/min. ^d The 5% weight loss temperature of polymers detected by the TGA analyses under nitrogen at a heating rate of 20 °C/min. ^e The best poling temperature. ^f Film thickness. ^g Second harmonic generation (SHG) coefficient. ^h The nonresonant d_{33} values calculated by using the approximate two-level model. ⁱ Order parameter $\Phi = 1 - A_1/A_0$; A_1 and A_0 are the absorbances of the polymer film after and before corona poling, respectively.

Results and Discussion

Synthesis. Compound **2** was prepared by reaction of **1** and 2-chloroethanol. It is a very simple reaction, and there are many literatures concerned with the reaction of aniline, the analogue of **1**, with 2-chloroethanol.¹³ However, compound **2** was not easy to obtain. We tried to synthesize compound **2** according to the previous literature, and the results are summarized in Table 1. Considering the yields and the purification status, we chose *t*-BuOH as the solvent, while the base was potassium carbonate with potassium iodide as the catalyst.

Chromophores **6–9** were synthesized through the normal azo coupling reaction with satisfied yields, in which chromophores **7** and **9** were important starting materials for the further preparation of chromophores **14–17**. 3-*N*-(*n*-butane)carbazole boronic acid (**12**) was obtained through three steps as shown in Scheme 1, while phenylboronic acid (**10**) was purchased from Aldrich directly. Under the typical conditions of Suzuki reaction,¹⁴ the syntheses of chromophores **14–17** were conveniently realized (Scheme 1). Generally, the Suzuki coupling reaction was used to be applied in the field of organic/polymeric light-emitting diodes, and here this reaction was handled for the preparation of NLO chromophores. Actually, we have tried to introduce bulky isolation spacer moieties to chromophore **7** or **9** by other methods, for example, Heck coupling reactions, but the resultant reaction mixture was very difficult to be isolated, and the yields were very low. As the conditions of Suzuki coupling reaction were mild, the target chromophores were obtained with high yields. Just by changing the boronic acid reagents, we could introduce different isolation groups to NLO chromophores. To further increase the bulkiness of the isolation group, we designed chromophores **21** and **22**, which were synthesized from the similar Suzuki reaction while 9,9-dihexylfluorene-2,7-bis(trimethyleneborate) was used instead of **12** or **13**, and chromophore **19** or **20** was used as another starting reagent (Scheme 3). Chromophores **21** and **22** could also be considered as “H”-type chromophores, in which the fluorene moieties were nearly perpendicular to the two phenyl rings of the azo moieties, acting as good bulky isolation groups. Then now, the isolation groups could be modified from hydrogen atoms, bromine atoms to phenyl, carbazolyl groups, and then to H-type chromophores with two azo chromophores linked together by a fluorene group. In this trend, the size of the isolation moieties becomes larger, but the total synthetic route is very simple while Suzuki coupling reactions were used. Therefore, it is convenient to compare the resultant NLO properties with different sizes of isolation groups.

The target polymers **P1–10** were easily synthesized from the corresponding chromophores and TDI under similar conditions as reported in the literature for the preparation of polyurethanes.¹¹ The convenient syntheses of polymers combined with their moderate glass transition temperature and the strong secondary forces between polymer chains make it not difficult to study the relationship between the structure of chromophore moieties and the NLO properties of the resultant polymers.

Structural Characterization. The chromophores and polymers were characterized by spectroscopic methods, and all give satisfactory spectral data (see Experimental Section and Table 2 for detailed analysis data). The NLO chromophores are new compounds, except chromophores **6** and **8**. Polymers **P2–P4** and **P6–P10** were not reported yet, while polymers **P1** and **P5** were prepared here for comparison. Figure S1 shows the IR spectra of chromophores **6**, **7**, **14**, **15**, and **21**, in which the absorption bands associated with the nitro groups are at about 1331 and 1510 cm⁻¹. After these chromophores reacting with TDI, the absorption bands of the nitro groups remained in the IR spectra of the resultant polymers **1–4** and **9** (Figure S2), while another strong absorption peak appears at about 1729 cm⁻¹, which is attributed to the vibration of the carbonyl group in a urethane group, indicating the formation of urethane linkages during the polymerization process as shown in Schemes 2 and 3. Similar results were also observed in the case of chromophores **8–9**, **16–17**, and **22** and their corresponding polymers **5–8** and **10** with the sulfonyl groups as the acceptor units in the chromophore moieties, and their IR spectra are shown in Figure S3 and S4.

In all the ¹H NMR spectra of the polymers **1–10**, the chemical shifts are consistent with the proposed polymer structure as demonstrated in Schemes 2 and 3, however, showing an inclination of signal broadening due to polymerization. For example, Figure S5 shows the spectra of chromophore **15** and the corresponding polymer **P4**, which were conducted in different solvents for their different solubility. It is obvious that there are some small peaks present downfield besides those signals derived from the chromophore moieties. These peaks are assigned to the urethane unit formed in the polymerization process,¹¹ confirming the successful polymerization between chromophore **15** and TDI.

All the polymers are soluble in common polar organic solvents such as THF, DMF, and DMSO. Their solutions can be easily spin-coated into thin solid films; therefore, it is convenient to test their NLO properties based on the thin films. The UV–vis absorption spectra of the chromophores and

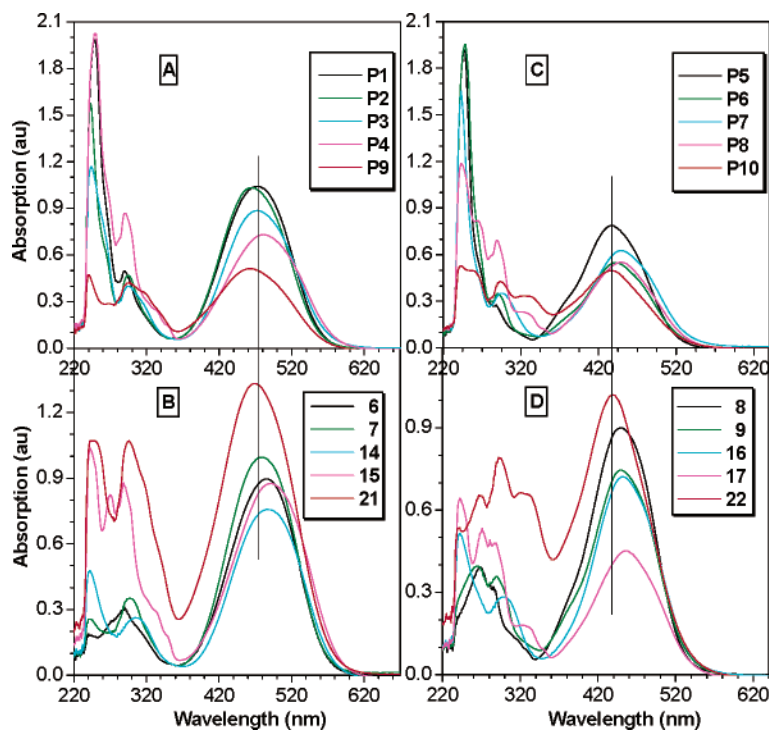


Figure 1. UV-vis spectra of THF solutions of (A) **P1–4** and **P9**, (B) chromophores **6**, **7**, **14**, **15**, and **21**, (C) **P5–8** and **P10**, (D) chromophores **8**, **9**, **16**, **17**, and **22**. Concentration: 0.02 mg/mL for polymers; 2.5×10^{-5} mol/L for small molecules.

polymers are shown in Figure 1, and the maximum absorption wavelength for the $\pi-\pi^*$ transition of the azo moieties in them are listed in the Experimental Section and Table 2. It is easily seen that after being bonded to the polymer chain the maximum absorption wavelength of the chromophore moieties were blue-shifted (up to 15 nm in the case of **P2**) compared with those of the free chromophore molecules.

The phenomena were reported previously, indicating the presence of the electronic interaction between the chromophore moieties and the polymer chain.¹¹ It is also noticed that the maximum absorption wavelengths of the two series of chromophores with nitro or sulfonyl groups as acceptor moieties are different. This is understandable: the introduced isolation groups, which were linked to the meta position of the amino group in the donor side, influenced the electronic structure of the total chromophore to some degree and led to the different absorptions. However, the effect is minor since the difference of wavelength is very little (less than 7 nm). As to the two “H”-type chromophores, there are two azo moieties in one molecule, which are linked together through a fluorene bridge, and the whole molecule could be considered as a new conjugated system to some degree, which has not been reported previously and needs to be further investigated. And actually, as reported in the literature, even the isolation moieties were not linked to the benzene ring directly; for example, if there is a methylene group between the isolation groups and the benzene ring, the maximum absorption of the resultant chromophore moieties would be different (up to 29 nm)³ due to the different surroundings environments, such as the polarizability and dielectric constant. Thus, the little difference in the maximum absorption wavelength of the chromophores with different isolation groups may indicate their minor difference in NLO properties.

The molecular weights of polymers were determined by gel permeation chromatography (GPC) with DMF as an eluent and polystyrene standards as calibration standards. All the results are summarized in Table 2, and most of the polymers possess similar molecular weight, which would perhaps facilitate the

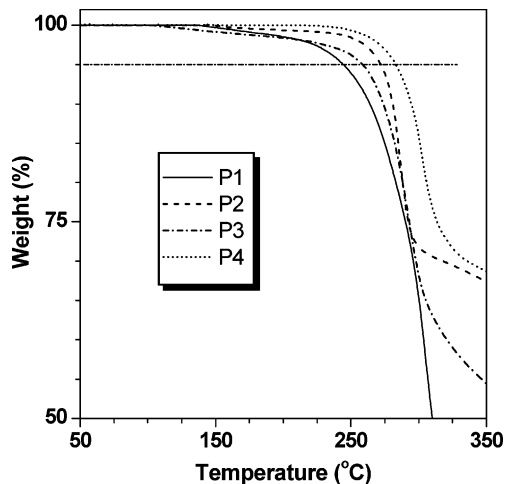


Figure 2. TGA thermograms of **P1–4** measured in air at a heating rate of 20 °C/min.

comparison of their properties on the same level. The molecular weight of **P7** is relatively low; this might be due to the relatively short reaction time. The polymers are thermally stable. Their TGA thermograms are shown in Figure 2 and Figure S6, and the 5% weight loss temperature of polymers are listed in Table 2. **P4** and **P8** exhibited better thermal stability than other polymers, indicating that the introduction of the carbazoyl group to the chromophore would benefit its stability against heating. The 5% weight loss temperature of **P7** is much lower than those of other polymers; this might be due to its lower molecular weight. The glass transition temperatures (T_g) of the polymers were investigated using a differential scanning calorimeter (Table 2), and polymers generally have moderate T_g about 140 °C due to the strong secondary forces between polymer chains and the electronic interaction between the chromophore moieties and the polymer chain. The relatively lower T_g of **P7** might also be caused by its low molecular weight.

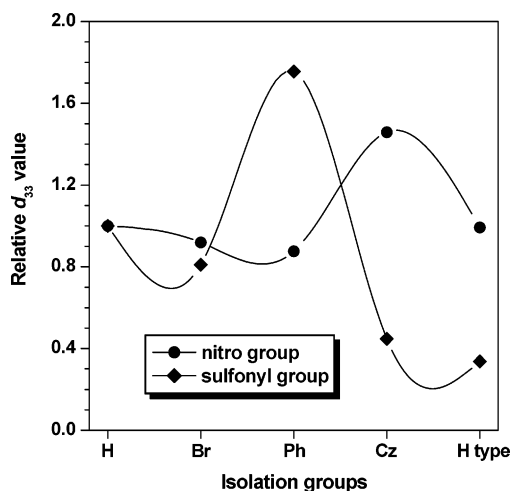


Figure 3. Comparison of the d_{33} values of the polymers using **P1** and **P5** as references respectively for the two series of polymers with either nitro or sulfonyl groups as acceptor groups in the chromophore moieties with different isolation groups. “Cz” represents carbazoyl groups, and “H type” is the isolation groups in chromophore **21** or **22**.

NLO Properties. To evaluate the NLO activity of the polymers, their poled thin films are prepared. The most convenient technique to study the second-order NLO activity is to investigate the second harmonic generation (SHG) processes characterized by d_{33} , an SHG coefficient. To check the reproducibility of the results, we repeated the measurements several times for each sample. The method for the calculation of the SHG coefficients (d_{33}) for the poled films has been reported in our previous papers.⁹ From the experimental data, the d_{33} values of **P1**–**10** are calculated at 1064 nm fundamental wavelength (Table 2). Generally, the d_{33} value of the same NLO polymer can be different when measured by different methods or different testing systems at different times. To avoid the above-mentioned possible deviations, the NLO properties of all the polymers were tested at the same time.

It is not strange that the 10 polymers show different d_{33} values for their different structure. However, it seems that there are no rules present in the tested results at the first glance. Figure 3 shows the comparison of the d_{33} values of the polymers using **P1** and **P5** as references respectively for the two series of polymers with nitro or sulfonyl groups as acceptor groups in the chromophore moieties. It is seen that the d_{33} values are not always increasing as the isolation groups enlarged, and for the sulfonyl groups as acceptor moieties, the d_{33} value reaches the peak value while the isolation group is phenyl moieties. However, carbazoyl groups are the best isolation moieties for the nitro groups. Since we would like to focus on the discussion of the relationship between the isolation groups and the resultant d_{33} values of the obtained polymers, we supposed that the introduction of different isolation groups would not influence the β values of the chromophores in a large degree. Actually, from their UV–vis spectra, the similar maximum absorption due to the π – π^* transition of the azo moieties indicates that different isolation groups do not heavily affect their electronic structure; then it is reasonable to ignore the possible difference stemmed from the β values of the chromophores. However, the introduction of different isolation groups would surely lead to the different molar weights of the obtained chromophores. According to the one-dimensional rigid orientation gas model¹⁵

$$d_{33} = \frac{1}{2} N \beta f^2 \omega (f^\omega)^2 \langle \cos^3 \theta \rangle \quad (1)$$

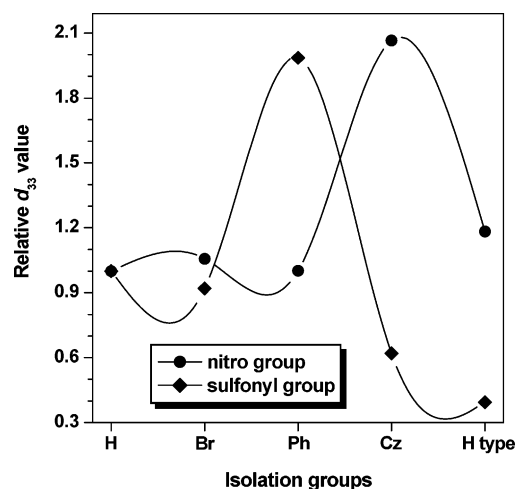


Figure 4. Comparison of the calculated d_{33} values, which were obtained by using the tested d_{33} values dividing the concentration of the active chromophore moieties, of the polymers using **P1** and **P5** as references respectively for the two series of polymers with nitro or sulfonyl groups as acceptor groups in the chromophore moieties. “Cz” represents carbazoyl groups, and “H type” is the isolation groups in chromophore **21** or **22**.

where N is the number density of the chromophore, β is its first hyperpolarizability, f is the local field factor, 2ω is the double frequency of the laser, ω is its fundamental frequency, and $\langle \cos^3 \theta \rangle$ is the average orientation factor of the poled film. As discussed above, supposing that the chromophores exhibit similar first hyperpolarizability, then under identical experimental conditions d_{33} should be proportional to the number density of the chromophore moieties in the polymers. Therefore, we considered the different concentrations of the active chromophore moieties in the polymers, using the tested d_{33} values dividing the concentration of the active chromophore moieties (the green part in the structure of the polymers as shown in Schemes 2 and 3) in the polymers, and compared the results again with those of **P1** and **P5** as references.

Figure 4 demonstrates the comparison of the calculated d_{33} values of the polymers. Similar to the results shown in Figure 3, for the sulfonyl groups as acceptor moieties, the d_{33} value reaches the peak value while the isolation group is phenyl moieties, and for the nitro groups, carbazoyl groups are the best isolation moieties. Then it is obvious that for a special NLO chromophore the d_{33} values of the resultant polymers are not always increasing as the isolation groups enlarged, even only considering the concentration of the active chromophore moieties in the system. This is understandable. As we know, the push–pull NLO chromophores with large dipole moments tend to compactly pack in a centrosymmetric manner due to the strong intermolecular dipole–dipole interactions, making poling-induced noncentrosymmetric alignment of chromophores a daunting task. And the purpose of controlling the shape of the chromophores or introducing isolation groups is to minimize the strong intermolecular dipole–dipole interactions to some degree to improve the d_{33} values of the materials. And in our case, we also would like to minimize this interaction by using different isolation groups. However, the addition of the isolation groups would increase the bulky of the resultant chromophore moieties, which makes the noncentrosymmetric alignment of the chromophores in the electronic field more difficult. That is to say, the introduction of the isolation groups mainly has two effects on the resultant d_{33} value of the material: on one hand, minimizing the interaction of the chromophores to improve the d_{33} value (named as good effect, abbreviated as G); on the

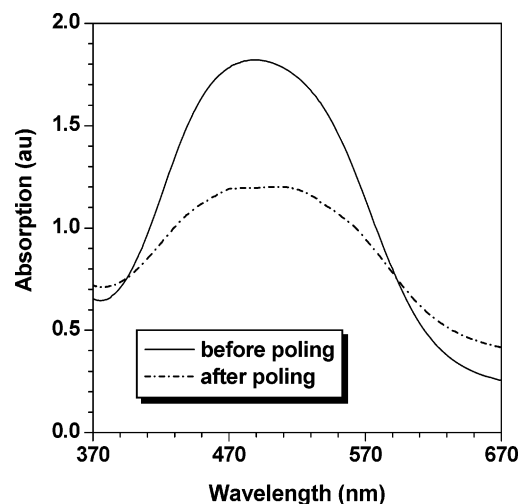


Figure 5. Absorption spectra of P4 before and after poling.

other hand, restraining the orderly alignment of the chromophores to decrease the d_{33} value (named as bad effect, abbreviated as B). So, there should be a balance between the two effects. Here in our case the only difference between the two series of the polymers is the different acceptor groups: one is nitro groups, another is sulfonyl moieties, and nitro groups are a stronger acceptor than sulfonyl moieties. Then, the intermolecular dipole–dipole interactions between the chromophores containing nitro groups as acceptors should be stronger than that present in the case of sulfonyl moieties. Also, at the same poling conditions, the force for the orderly alignment of the chromophore with sulfonyl moieties as acceptor groups should be weaker than that for the nitro groups. Therefore, to minimize the interaction of the nitro chromophores to a similar degree as in the case of sulfonyl chromophores, the isolation groups should be larger. And on the other hand, to restrain the alignment of the nitro groups in the electronic field during the poling process to the similar extent as in the case of the sulfonyl chromophore, the introduced isolation groups also should be larger. Thus, the two effects, G and B, should be much different when the chromophores are different. When the isolation groups were very small, such as bromine atoms in the two cases of chromophores and phenyl groups in the case of the nitro chromophores, the G and B effects are not obvious, so the NLO properties are similar as those of hydrogen atoms as isolation groups (or considering that there are no isolation groups); when the isolation groups are moderate, such as the phenyl groups in the case of the sulfonyl chromophores and the carbazolyl groups in the case of the nitro chromophores, the G effect is obvious while the B effect is negligible, so the NLO properties are much better; but when the isolation groups are even larger, such as in the cases of P8–10, the G effect is still good or even better; however, the B effect does work now, cancels the G effect to some degree, and leads to the worse NLO results. It should be pointed out that the above-discussed NLO properties of polymers are the values tested from the experiment directly. If considered the resonant enhancement due to the absorption of the chromophore moieties at 532 nm, the NLO properties should be smaller as shown in Table 2 ($d_{33(\infty)}$), which were calculated by using the approximate two-level model. However, the trends existing in the $d_{33(\infty)}$ values were similar as we discussed in the test d_{33} values of the polymers.

To further explore the alignment of the chromophore moieties in the polymers, we measured their order parameter (Φ). Figure 5 shows the UV–vis spectrum of the film of P4 before and after corona poling as an example. Those spectra of other

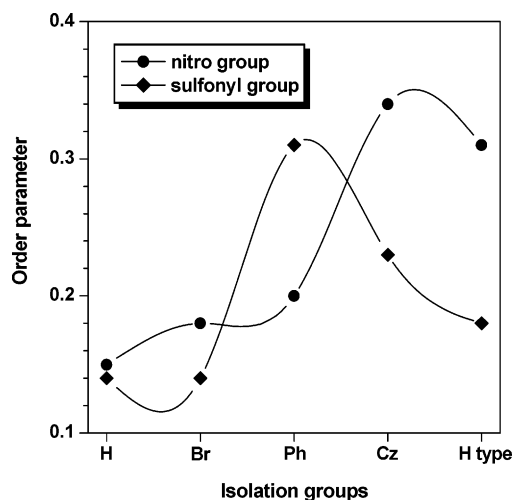


Figure 6. Order parameter (Φ) of polymers, which were calculated from the equation $\Phi = 1 - A_1/A_0$; A_1 and A_0 are the absorbances of the polymer film after and before corona poling, respectively.

polymers are demonstrated as Figure S7–S15 in the Supporting Information. After the corona poling, the dipole moments of the chromophore moieties in the polymers were aligned, and the absorption curves decreased due to birefringence.

From the absorption change, the Φ value for the polymers can be calculated according to the following equation:

$$\Phi = 1 - A_1/A_0 \quad (2)$$

where A_1 and A_0 are the absorbances of the polymer film after and before corona poling, respectively. The calculated Φ values are summarized in Table 2. Figure 6 also describes the results more visually directly. As we analyzed above, the Φ value increases until a peak point with the isolation groups enlarging and then decreases while the isolation groups become even bigger. That is to say, for a given chromophore moiety, there should be a suitable isolation group present to balance the G and B effects, and introducing this isolation group to the chromophore moieties would boost the microscopic β value of the chromophore to possibly higher macroscopic NLO property of the polymers containing these chromophore moieties efficiently. From this point, perhaps, the reported NLO polymers with dendronized chromophore as side chains might achieve even better NLO properties if more suitable isolation groups were used.

It should be pointed out that in our case the phenyl and carbazolyl groups are suitable isolation groups for the sulfonyl and nitro chromophores, respectively, but this is not meant that in any case the two groups are suitable isolation groups for the two kinds of chromophores. We must pay attention to the linked position of the isolation groups. And actually, in the other case, the NLO properties could be even boosted to much higher by using the same nitro chromophore with applying the site isolation principle.^{9c} However, our preliminary results demonstrated that for a given chromophore, and at the given linkage position, there is really a relationship present between the bulky of the isolation group and the resultant NLO effect. And to study the structure–property relationship of NLO polymers in detail, to realize the widely practical application of NLO materials, it is needed to notice the adjustment of the size of the isolation groups linked to the chromophore moieties. Further study is still underway in our lab.

The dynamic thermal stabilities of the NLO activities of the polymers are investigated by depoling experiments, in which

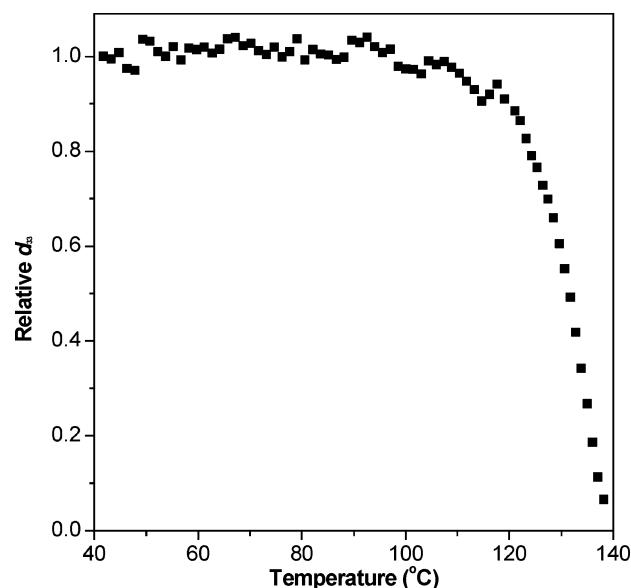


Figure 7. Decay of SHG coefficient of P8 as a function of temperature.

the real-time decays of their SHG signals are monitored as the poled films are heated from 35 to 180 °C in air at a rate of 4 °C/min. The results indicated that the long-term temporal stability of most of the polymers are relatively good, and the introduction of the large size of the isolated groups to the sulfonyl-based chromophores benefits the thermal stability of the resultant polymers. Figure 7 showed the decay of SHG coefficient of P8 as a function of temperature; the onset temperature for decays is found to be as high as 121 °C, much better than that of P5 without isolation groups. Other decay curves for the polymers were listed as Figure S16–S24 in the Supporting Information. The behavior of the polymers with nitro groups in their chromophore moieties is different from the polymers containing sulfonyl-based chromophores; the introduction of the isolation groups does not benefit the stability of their NLO effect, but leads to the lower onset temperature. However, most of the polymers showed stable NLO properties up to 120 °C, making them good candidates for the practical applications.

Conclusions

Two series of polyurethanes containing dendronized NLO chromophores as side chains were prepared, in which the size of isolation groups changed from small atoms to much larger groups such as carbazolyl groups. The obtained 10 polymers were soluble in common polar solvents and well characterized. Our preliminary study demonstrates the following:

1. The NLO properties of the corresponding polymers do not always increase accompanying the enlargement of the isolation groups linked to the chromophore moieties. Similar phenomena are also found in the case of the poling efficiency of the polymers.

2. The same isolation group would lead to different effects in different NLO chromophores. If the NLO chromophores are different, different results would be obtained even though the same isolation group linked. That is to say, for a given chromophore moiety and given linkage position, there should be a suitable isolation group present to boost its microscopic β value to possibly higher macroscopic NLO property efficiently.

Thus, our study may provide some useful information on the design of new NLO polymers and be helpful to obtain even better NLO properties by using the present chromophores.

Acknowledgment. We are grateful to the National Science Foundation of China (No. 20402011), the National Fundamental Key Research Program, and Hubei Province for financial support.

Supporting Information Available: Figures of FT-IR spectra, ^1H NMR spectra, and absorption spectra of polymers before and after poling; decay curves of SHG coefficients of polymers as a function of temperature. This material is available free of charge via the Internet at <http://pubs.acs.org>.

References and Notes

- (1) (a) Lee, M.; Katz, H. E.; Erben, C.; Gill, D. M.; Gopalan, P.; Heber, J. D.; McGee, D. J. *Science* **2002**, 298, 1401. (b) Shi, Y.; Zhang, C.; Zhang, H.; Bechtel, J. H.; Dalton, L. R.; Robinson, B. H.; Steier, W. H. *Science* **2000**, 288, 119. (c) Burland, D. M.; Miller, R. D.; Walsh, C. A. *Chem. Rev.* **1994**, 94, 31. (d) Ma, H.; Jen, A. K. Y. *Adv. Mater.* **2001**, 13, 1201. (e) Moerner, W. E.; Jepsen, A. G.; Thompson, C. L. *Annu. Rev. Mater. Sci.* **1997**, 32, 585. (f) Barclay, G. G.; Ober, C. K. *Prog. Polym. Sci.* **1993**, 18, 899.
- (2) (a) Marks, T. J.; Ratner, M. A. *Angew. Chem., Int. Ed. Engl.* **1995**, 34, 155. (b) Marder, S. R.; Kippelen, B.; Jen, A. K. Y. Peyghambarian, N. *Nature (London)* **1997**, 388, 845. (c) Zyss, J. *Nonlinear Opt.* **1991**, 1, 3. (d) Bai, Y.; Song, N.; Gao, J. P.; Sun, X.; Wang, X.; Yu, G.; Wang, Z. Y. *J. Am. Chem. Soc.* **2005**, 127, 2060. (e) Andreu, R.; Blesa, M. J.; Carrasquer, L.; Garin, J.; Orduna, J.; Villacampa, B.; Alcala, R.; Casado, J.; Delgado, M. C. R.; Navarrete, J. T. L.; Allain, M. *J. Am. Chem. Soc.* **2005**, 127, 7282. (f) Wang, Q.; Wang, L. M.; Yu, L. P. *Macromol. Rapid Commun.* **2000**, 21, 723.
- (3) (a) Dalton, L. R.; Harper, A. W.; Ren, A.; Wang, F.; Todorova, G.; Chen, J.; Zhang, C.; Lee, M. *Ind. Eng. Chem. Res.* **1999**, 38, 8. (b) Marder, S. R.; Cheng, L. T.; Tiemann, B. G.; Friedli, A. C.; Blanchard-Desce, M.; Perry, J. W.; Skindhøj, J. *Science* **1994**, 263, 511. (c) Luo, J. D.; Ma, H.; Haller, M.; Barto, R. R. *Chem. Commun.* **2002**, 8, 888.
- (4) (a) Robinson, B. H.; Dalton, L. R. *J. Phys. Chem. A* **2000**, 104, 4785. (b) Robinson, B. H.; Dalton, L. R.; Harper, H. W.; Ren, A.; Wang, F.; Zhang, C.; Todorova, G.; Lee, M.; Anisfeld, R.; Garner, S.; Chen, A.; Steier, W. H.; Houbrecht, S.; Persoons, A.; Ledoux, I.; Zyss, J.; Jen, A. K.-Y. *Chem. Phys.* **1999**, 245, 35. (c) Dalton, L. R.; Steier, W. H.; Robinson, B. H.; Zhang, C.; Ren, A.; Garner, S.; Chen, A.; Londergan, T.; Irwin, L.; Carlson, B.; Fifield, L.; Phelan, G.; Kincaid, C.; Amend, J.; Jen, A. K.-Y. *J. Mater. Chem.* **1999**, 9, 19.
- (5) (a) Fréchet, J. M. J. *Proc. Natl. Acad. Sci. U.S.A.* **2002**, 99, 4782. (b) Fréchet, J. M. J.; Henmi, M.; Gitsov, I.; Aoshima, S.; Leduc, M. R.; Grubbs, R. B. *Science* **1995**, 269, 1080. (c) Fréchet, J. M. J.; Hawker, C. J.; Gitsov, I.; Leon, J. W. *J. Macromol. Sci., Pure Appl. Chem.* **1996**, A33, 1399. (d) Hecht, S.; Fréchet, J. M. J. *Angew. Chem., Int. Ed.* **2001**, 40, 74.
- (6) (a) Luo, J.; Haller, M.; Li, H.; Tang, H.; Jen, A. K.-Y.; Jakka, K.; Chou, C.-H.; Shu, C.-F. *Macromolecules* **2004**, 37, 248. (b) Ma, H.; Liu, S.; Luo, J.; Suresh, S.; Liu, L.; Kang, S. H.; Haller, M.; Sassa, T.; Dalton, L. R.; Jen, A. K.-Y. *Adv. Funct. Mater.* **2002**, 12, 565. (c) Ma, H.; Chen, B. Q.; Sassa, T.; Dalton, L. R.; Jen, A. K.-Y. *J. Am. Chem. Soc.* **2001**, 123, 986.
- (7) (a) Haller, M.; Luo, J.; Li, H.; Kim, T. D.; Liao, Y.; Robinson, B. H.; Dalton, L. R.; Jen, A. K. Y. *Macromolecules* **2004**, 37, 688. (b) Luo, N.; Wang, D. N.; Ying, S. K. *Macromolecules* **1997**, 30, 4405. (c) Zhang, C.; Wang, C.; Dalton, L. R.; Zhang, H.; Steier, W. H. *Macromolecules* **2001**, 34, 253. (d) Suresh, S.; Gulotty, R. J.; Bales, S. E.; Inbasekaran, M. N.; Chartier, M. A.; Cummins, C.; Smith, D. W. *Polymer* **2003**, 44, 5111.
- (8) (a) Dalton, L. R. *Pure Appl. Chem.* **2004**, 76, 1421. (b) Sullivan, P. A.; Akelaitis, A. J. P.; Lee, S. K.; McGrew, G.; Lee, S. K.; Choi, D. H.; Dalton, L. R. *Chem. Mater.* **2006**, 18, 344. (c) Luo, J.; Haller, M.; Ma, H.; Liu, S.; Kim, T. D.; Tian, Y.; Chen, B.; Jang, S. H.; Dalton, L. R.; Jen, A. K. Y. *J. Phys. Chem. B* **2004**, 108, 8523.
- (9) (a) Li, Z.; Qin, J.; Li, S.; Ye, C.; Luo, J.; Cao, Y. *Macromolecules* **2002**, 35, 9232. (b) Li, Z.; Huang, C.; Hua, J.; Qin, J.; Yang, Z.; Ye, C. *Macromolecules* **2004**, 37, 371. (c) Li, Z.; Qin, A.; Lam, J. W. Y.; Dong, Y.; Dong, Y.; Ye, C.; Williams, I. D.; Tang, B. Z. *Macromolecules* **2006**, 39, 1436. (d) Luo, J.; Qin, J.; Kang, H.; Ye, C. *Chem. Mater.* **2001**, 13, 927. (e) Li, Z.; Hua, J.; Li, Q.; Huang, C.; Qin, A.; Ye, C.; Qin, J. *Polymer* **2005**, 46, 11940. (f) Gong, W.; Li, Q.; Li, Z.; Lu, C.; Zhu, J.; Li, S.; Yang, J.; Cui, Y.; Qin, J. *J. Phys. Chem. B* **2006**, 110, 10241.
- (10) (a) Yu, D.; Gharavi, A.; Yu, L. *J. Am. Chem. Soc.* **1995**, 117, 11680. (b) Wang, X.; Li, L.; Chen, J. I.; Marturankul, S.; Kumar, J.; Tripathy, S. K. *Macromolecules* **1997**, 30, 219. (c) Woo, H. Y.; Shim, H. K.; Lee, K. S.; Jeong, M. Y.; Lim, T. K. *Chem. Mater.* **1999**, 11,

218. (d) Ulman, A.; Willand, C. S.; Kohler, W.; Robello, D. R.; Williams, D. J.; Handley, L. *J. Am. Chem. Soc.* **1990**, *112*, 7083. (e) Sohn, J.; Park, S. Y.; Moon, H.; Mun, J.; Yoon, C. S. *React. Funct. Polym.* **2000**, *45*, 109.
- (11) (a) Woo, H. Y.; Shim, H. K.; Lee, K. S. *Macromol. Chem. Phys.* **1998**, *199*, 1427. (b) Park, C. K.; Zieba, J.; Zhao, C. F.; Swedek, B.; Wijekoon, W. M. E. P.; Prasad, P. N. *Macromolecules* **1995**, *28*, 3713. (c) Lee, J. Y.; Bang, H. B.; Park, E. J.; Lee, W. J.; Rhee, B. K.; Lee, S. M. *Polym. Int.* **2004**, *53*, 1838. (d) Tsutsumi, N.; Matsumoto, O.; Sakai, W. *Macromolecules* **1997**, *30*, 4584. (e) Moon, K. J.; Shim, H. K.; Lee, K. S.; Zieba, J.; Parasad, P. N. *Macromolecules* **1996**, *29*, 861.
- (12) (a) Lao, W.; You, J.; Yu, Z.; Qu, Q. *HuaXue ShiJi* **2000**, *22*, 260. (b) Courtin, A. *Helv. Chim. Acta* **1983**, *66*, 1046.
- (13) (a) Samyn, C.; Verbiest, T.; Kester, E.; Broeck, K. V. D.; Beylen, M. V.; Persoons, A. *Polymer* **2000**, *41*, 6049. (b) Tsutsumi, N.; Matsumoto, O.; Sakai, W.; Kiyotsukuri, T. *Macromolecules* **1996**, *29*, 592. (c) Thomas, S. W.; Swager, T. M. *Macromolecules* **2005**, *38*, 2716.
- (14) Suzuki, A.; Miyaoura, N. *Chem. Rev.* **1995**, *95*, 2457.
- (15) Moylan, C. R.; Miller, R. D.; Twieg, R. J.; Lee, V. Y.; McComb, I. H.; Ermer, S.; Lovejoy, S. M.; Leung, D. S. *Proc. SPIE* **1995**, *2527*, 150.

MA0608875